Antiviral Research 99 (2013) 18–26

Contents lists available at SciVerse ScienceDirect

Antiviral Research

journal homepage: www.elsevier.com/locate/antiviral

Synthesis and evaluation of a new phosphorylated ribavirin prodrug

Steven D. Dong [a,*], Chin-Chung Lin [a], Mel Schroeder [b]

[a] Epiphany Biosciences, Inc., San Francisco, CA 94111, United States
[b] Kalexsyn, Inc., 4502 Campus Drive, Kalamazoo, MI 49008, United States

ARTICLE INFO

Article history:
Received 6 September 2012
Revised 12 April 2013
Accepted 15 April 2013
Available online 24 April 2013

Keywords:
Ribavirin
Prodrug
Antiviral drug
Hepatitis C virus
Red blood cell
Cellular uptake

ABSTRACT

Ribavirin is an important broad-spectrum antiviral drug. However, its utilization can be limited by its potential to cause hemolytic anemia as well as its variability in dosing levels and efficacy outcomes. To overcome these issues, we report on a new alkoxyalkylphosphodiester prodrug of ribavirin (**2**) that is designed to release the active ribavirin-monophosphate species selectively in nucleated cells while limiting its exposure in anucleated red blood cells (RBCs). Prodrug **2** displays improved *in vitro* antiviral activity against the hepatitis C virus replicon and influenza virus. Unlike ribavirin, prodrug **2** does not significantly decrease ATP levels in RBCs. Prodrug **2** demonstrates decreased uptake in RBCs but increased uptake in HepG2 hepatocytes when compared to ribavirin. *In vivo*, prodrug **2** is orally bioavailable and well-tolerated in rats in which it is processed to ribavirin and accumulates in the liver. These results indicate that prodrug **2** has the potential for safer, lower, less frequent, and less variable administration than ribavirin.

1. Introduction

Ribavirin was first disclosed in 1972 but still remains the only approved small molecule antiviral drug with broad-spectrum activity against both RNA and DNA viruses (Sidwell et al., 1972). Clinically, ribavirin is used to treat hepatitis C virus (HCV) in combination with peginterferon, respiratory syncytial virus, and Lassa fever virus infections (Crotty et al., 2002). Recent data suggest that ribavirin may continue to play a role in reducing relapse and enhancing a sustained virological response in future therapeutic modalities to treat HCV infection (Feld, 2012; Pockros, 2010; Shiffman, 2009).

Despite its clinical utility, ribavirin's mechanism of action has remained enigmatic (Parker, 2005). Its antiviral activity has been attributed to both direct and indirect mechanisms that target a variety of viral and host enzymes, which utilize purine nucleoside or nucleotide as a substrate or cofactor. It is well recognized that ribavirin must be phosphorylated to become pharmacologically active.

A limitation to the clinical utility of ribavirin is that it can induce hemolytic anemia (Russmann et al., 2006). Ribavirin is actively transported into red blood cells (RBCs) by equilibrative nucleoside transporter 1 (ENT1) on the plasma membrane and is subsequently metabolized to various phosphorylated derivatives (Page and Connor, 1990). Since RBCs lack phosphatases, the resulting phosphorylated ribavirin species become trapped intracellularly and accumulate, resulting in very high intra-RBC concentrations that can exceed 1 mM (Inoue et al., 2006). The high intracellular ribavirin concentrations in RBCs competitively deplete ATP levels, which leads to hemolytic anemia.

Additionally, recent studies suggest that ENT1-mediated uptake of ribavirin in hepatocytes may play a pivotal role in its antiviral effectiveness (Bengsch and Thimme, 2010; Ibarra and Pfeiffer, 2009; Iikura et al., 2012). The variability in HCV patient response to ribavirin may be due in part to the existence of different ENT1 isoforms in human hepatocytes and their varying capacities to transport ribavirin (Fukuchi et al., 2010). Therefore, a ribavirin analog that does not solely depend on ENT1 uptake in hepatocytes may have a more uniform effect in patients expressing different isoforms.

We sought to develop a new prodrug of ribavirin that would have the potential for improved efficacy, safety, and dosing. Since ribavirin's mechanism(s) of action requires phosphorylation, our first consideration was the pre-installation of a phosphate group so that the active species could be directly introduced to infected cells and bypass the rate-limiting phosphorylation to ribavirin-monophosphate (**1**, Fig. 1). Unprotected phosphorylated compounds do not readily cross cell membranes, so a suitable prodrug approach was required (He et al., 2007). Hostetler et al. have previously reported an alkoxyalkylphosphonate ester prodrug approach to improve the bioavailability of acyclic nucleoside phosphorous containing drugs such as cidofovir (Hostetler, 2009, 2010; Hostetler et al., 2000, 2001). The long-chain

* Corresponding author. Address: Steven Dong, Epiphany Biosciences, 1 California Street, Suite 2800, San Francisco, CA 94111, United States. Tel.: +1 415 765 7193; fax: +1 415 765 7200.
E-mail address: steved@epiphanybio.com (S.D. Dong).

0166-3542/$ - see front matter © 2013 Elsevier B.V. All rights reserved.
http://dx.doi.org/10.1016/j.antiviral.2013.04.014

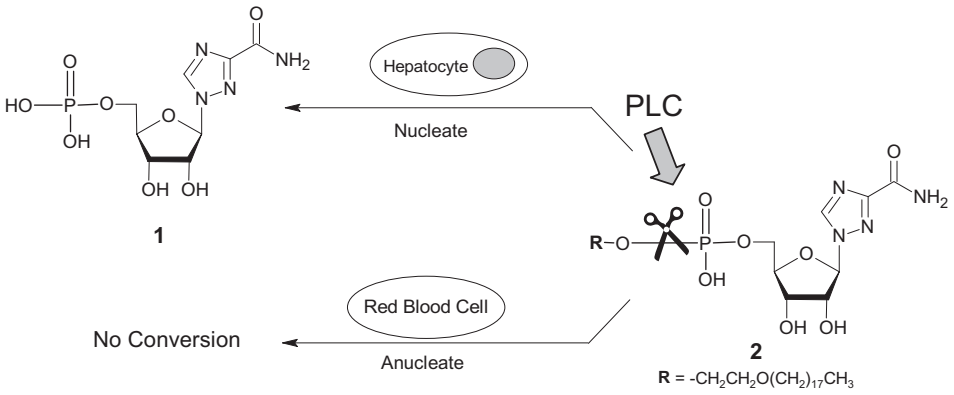

Fig. 1. Proposed mechanism of intracellular cleavage of octadecyloxyethyl ribavirin phosphodiester prodrug **2** by phospholipase C (PLC) yields ribavirin mono-phosphate (1) in nucleated cells such as hepatocytes containing PLC but not in anucleated cells such as red blood cells which do not have PLC.

alkoxyalkylphosphonate ester prodrug moiety mimics lysophospholipids which are readily taken up in the gastrointestinal tract and into cells. After being taken up in the cell, the alkoxyalkylphosphonate ester prodrug moiety is then cleaved by phospholipase C (PLC) to release the unprotected drug as the free phosphonic acid.

We hypothesized that a similar prodrug approach would be applicable to the ribavirin-monophosphate nucleotide **1** and could provide several advantages, most notably a differential prodrug activation profile in nucleated cells versus anucleated cells (Fig. 1). ^{1}H spin-echo NMR experiments in human RBC lysates demonstrated that PLC is not present in anucleated RBCs (Selle et al., 1992). Consequently, PLC-mediated cleavage of an alkoxyalkyl prodrug in RBCs is not possible. However, in nucleated cells such as hepatocytes where PLC is present, an alkoxyalkyl group can be cleaved to yield **1**. Direct introduction of the active species into target nucleated cells without concurrent processing in anucleated RBCs could result in an overall improved therapeutic index. Herein, we report a new ribavirin prodrug (**2**) and its preliminary *in vitro* and *in vivo* characterization.

2. Materials and methods

2.1. Compounds and radiochemicals

1-{5-O-[(2-chlorophenoxy)(octadecyloxy)phosphoryl]-2,3-O-isopropylidene-beta-D-ribofuranosyl}-1H-1,2,4-triazole-3-carboxamide (**4**). Triazole (0.146 g, 2.12 mmol), triethylamine (0.215 g, 2.12 mmol), and dry THF (2.1 mL) were added to 2-chlorophenyl phosphorodichloridate (0.259 g, 1.06 mmol) in dry THF (1.3 mL). The reaction was stirred at room temperature for 1 h, filtered, and washed with THF (2.1 mL). 2′,3′-Isopropylidene ribavirin (**3**, 0.226 g, 0.795 mmol, Toronto Research Chemicals; Toronto, ON, Canada) and 1-methylimidazole (0.084 mL, 1.06 mmol) in THF (1.2 mL) were added to the filtrate and stirred at room temperature for 1 h. 2-(octadecyloxy)ethanol (0.250 g, 0.795 mmol) was added, stirred at room temperature overnight, and concentrated *in vacuo*. Purification by flash chromatography (CH_2Cl_2 + 0 to 4% MeOH) and concentration *in vacuo* provided **4** as a colorless oil (0.439 g, 71%). See Supplementary Information for spectral characterization.

1-(5-O-{hydroxy[2-(octadecyloxy)ethoxy]phosphoryl}-2,3-O-isopropylidene-beta-D-ribofuranosyl)-1H-1,2,4-triazole-3-carboxamide (**5**). 1,1,3,3-tetramethylguanidine (0.378 g, 3.28 mmol) and syn-2-pyridinealdoxime (0.401 g, 3.28 mmol) in THF (4.2 mL) were added to a solution of **4** (0.448 g, 0.581 mmol) in THF (12.2 mL) and stirred at room temperature overnight. The reaction was concentrated *in vacuo*, and the residue was purified by flash chromatography (CH_2Cl_2 + 0 to 30% MeOH). Following concentration, the resulting material was partitioned between THF: EtOAc (1:1) and cold H_2O (pH 1–2), extracted thrice with THF: EtOAc, dried with Na_2SO_4 concentrated *in vacuo*, and azeotroped from MeOH to yield **5** as a white solid (0.312 g, 81%).

1-(5-O-{hydroxy[2-(octadecyloxy)ethoxy]phosphoryl}-beta-D-ribofuranosyl)-1H-1,2,4-triazole-3-carboxamide (**2**). Acetonide **5** (0.304 g, 0.460 mmol) was dissolved in TFA:H_2O (9:1, 4 mL) and stirred at room temperature for 45 min. The reaction was concentrated, azeotroped from toluene, suspended in MeOH, and concentrated thrice to produce prodrug **2** as a white solid (0.264 g, 93%).

5-[^{14}C]-ribavirin with a specific activity of 55.8 mCi/mmol was purchased from Moravek Biochemicals (Brea, CA). 5-[^{14}C]-**2** with a specific activity of 56.3 mCi/mmol was prepared from 5-[^{14}C]-ribavirin according to the previous methods.

2.2. In vitro assays

2.2.1. Antiviral assays

HCV antiviral activity was assessed according to a previously reported method in the stably HCV RNA-replicating cell line AVA5 (genotype 1b, subgenomic replicon) and APC103 (genotype 1a, subgenomic replicon) (Okuse et al., 2005; Blight et al., 2000). Compounds were added to dividing cultures daily for three days with cultures generally at 30–50% confluence at assay initiation and reaching confluence during the last day of treatment. Intracellular HCV RNA levels and cytotoxicity were assessed 72 h after treatment. Intracellular HCV RNA levels were measured using a conventional blot hybridization method in which HCV RNA was normalized to β-actin mRNA for each individual culture. Cytotoxicity was measured using a previously reported neutral red dye uptake assay (Korba and Gerin, 1992).

Anti-influenza A activity was determined against influenza A/Hong Kong/8/68 (ATCC; Manassas, VA) in Madin-Darby canine kidney (MDCK) cells (ATCC) using a previously reported colorimetric readout utilizing the CellTiter 96® AQueous One Solution Cell Proliferation Assay (Promega; Madison, WI) to determine virus-induced cytopathogenic effects (Fletcher et al., 2000). The MDCK cells were plated at 10,000 cells/well in 96 well plates with 2% serum as stationary monolayers for both antiviral and cytotoxicity assays. Cytotoxicity was measured using the previously reported CytoTox-ONE™ Homogeneous Membrane Integrity Assay (Promega).

2.2.2. Nucleotide pool assay

Huh-7.5 cells (Dr. Ralf Bartenschlager; University of Heidelberg, Germany) were incubated for 24 h with either ribavirin, prodrug **2**,

or dimethyl sulfoxide (DMSO) (vehicle control), and the resulting nucleotide pools were extracted and analyzed by HPLC according to methods previously described (NovoCIB S.A.S.; Lyon, France) (Randall et al., 2003; Di Pierro et al., 1995).

2.2.3. ATP level determination

Human RBCs were incubated with either 1 mM **2**, ribavirin, or DMSO (vehicle control) for 12 h employing previously disclosed conditions (De Franceschi et al., 2000). Just prior to ATP level determination, a vehicle control sample was spiked with 1 mM ribavirin to normalize the observed luminescence for any interference from ribavirin itself. ATP levels were quantified using the CellTiter-Glo® Luminescent Cell Viability Assay (Promega).

2.2.4. Uptake assays in RBCs and HepG2 cells

Uptake of [^{14}C]-**2** or 5-[^{14}C]-ribavirin into RBCs was determined using a previously reported approach (Lin et al., 2003). Whole blood was collected from human donors, the hematocrit (H) determined, and the RBCs separated from plasma by centrifugation. Plasma was spiked with the radiolabeled test article to achieve a target concentration of 100 μg (0.1 μCi)/mL in whole blood and gently mixed with blood cell suspension. Samples were incubated in duplicate for 0, 0.5, 1, 2, 4 and 24 h. RBCs were separated from plasma by centrifugation. Following RBC decolorization with H_2O_2, the concentration in the reconstituted blood (C_b) and plasma (C_p) was determined by liquid scintillation counting (LSC, PerkinElmer). The RBC concentration (C_{rbc}) was calculated as follows: $C_{rbc} = [C_b - C_p(1 - H)]/H$, and the ratios of $C_{rbc}/(C_{rbc} + C_p)$ and $C_p/(C_{rbc} + C_p)$ were calculated.

To determine uptake in a cultured hepatocyte line, HepG2 cells (50,000 cells/well; ATCC) were incubated with either 100 μg (0.1 μCi)/mL [^{14}C]-**2** or 5-[^{14}C]-ribavirin at 5% CO_2 and 37 °C for 24 h (Fig. 6). At various timepoints (0, 1, 2, 4, and 24 h), the supernatant was removed, cells were washed with cold PBS, and a total cell lysate was prepared. Radioactivity in the supernatant ($C_{Supernatant}$) and the cell lysate (C_{Hep}) was counted by LSC, and the ratio of $C_{Hep}/(C_{Hep} + C_{Supernatant})$ was calculated.

2.3. In vivo studies

2.3.1. Animal studies

The 28-day dosing study was conducted at Bridge Laboratories (Beijing, China), and the tissue distribution study was conducted at Xenometrics (Stilwell, KS). These test facilities were accredited by the Association for Assessment and Accreditation of Laboratory Animal Care International, and all protocols were approved by the facilities' respective Institutional Animal Care and Use Committees. All procedures involving animals were conducted humanely and were performed by or under the direction of trained and experienced personnel. These studies did not unnecessarily duplicate previous studies.

Sprague Dawley rats (Vital River Laboratory Animal Technology; Beijing, China) received either **2** (304.8 mg/kg/day) or ribavirin (120 mg/kg/day) daily by oral gavage for 28 consecutive days. Dosing formulations were prepared by dissolving an appropriate amount of test article into DMSO (10% of the final volume), adding 5% glucose injection (90% of the final volume), and homogenization. Blood samples from three non-fasted animals/group at each time point were collected on Days 1, 14, and 28 prior to dose and at 1, 3, and 6 h post-dose. Parameters evaluated included body weights and food consumption, and macroscopic pathology. Plasma was analyzed by LC/MS/MS (Supplementary Information).

For the tissue distribution studies, [^{14}C]-**2** was formulated in 40% (w/v%) hydroxypropyl-β-cyclodextrin in pH 7.4 buffer and administered to Sprague Dawley rats at 10 mg/kg by oral gavage with a total dosed radioactivity of approximately 20 μCi/kg. 5-[^{14}C]-Ribavirin was formulated in sterile water and was administered at 10 mg/kg with a total dosed radioactivity of approximately 225 μCi/kg. Blood samples were collected at 1 and 3 h into blood tubes containing K_3EDTA. An aliquot of whole blood was kept, and the remaining blood was centrifuged to separate the plasma and RBCs. Following the terminal sacrifice at 1 and 3 h, the entire liver and lungs were collected. Samples were homogenized and analyzed by LSC (Supplementary Information).

3. Results

3.1. Synthesis

A very efficient synthesis of **2** was developed from ribavirin (Fig. 2). The 2′,3′-protected ribavirin acetonide **4** was coupled with 2-chlorophenyl phosphorchloridate via the phosphotriester approach. In situ ester formation with hexadecyloxypropanol and 1′-methylimidazole produced phosphotriester **5**. Sequential deprotections provided the target prodrug **2** in 62.5% overall yield from **4** at >95% purity by HPLC.

3.2. In vitro studies

3.2.1. Antiviral activity against HCV and influenza A virus

Prodrug **2** was screened for *in vitro* activity against HCV and influenza virus. Prodrug **2** was approximately 10-fold more active than ribavirin against the HCV 1b replicon and 6-fold more active against the HCV 1a replicon. Prodrug **2** displayed an approximately 13–25-fold improved selectivity index compared to ribavirin in these assays (Table 1). Prodrug **2** also demonstrated an approximately 74-fold enhanced activity against influenza A virus compared to ribavirin (Table 1). The improvement in *in vitro* activity was consistent with the prodrug **2** being converted directly to the pharmacologically species **1**, thereby bypassing the rate-limiting phosphorylation step required by ribavirin.

3.2.2. Cellular GTP depletion

Inosine monophosphate (IMP) dehydrogenase controls the guanine nucleotide pool by catalyzing the conversion of IMP to xanthosine monophosphate, the pivotal step in guanine nucleotide biosynthesis. Inhibition of IMP dehydrogenase has been proposed as one of the mechanisms by which phosphorylated ribavirin **1** disrupts viral replication through interruption of host nucleotide biosynthesis and/or viral genome transcription/translation (Dixit and Perelson, 2006). We examined prodrug **2**'s effect on cellular GTP and nucleotide pool levels in a whole-cell assay (Fig. 3). Prodrug **2** depleted cellular guanine nucleotide pools in a dose-dependent manner. At a lower concentration of 30 μm, prodrug **2** reduced GTP levels similar to the more concentrated ribavirin control (100 μm). These results are consistent with **2** being released directly as the pharmacologically active species **1**.

3.2.3. ATP levels in RBCs

The effect of prodrug **2** on ATP levels in RBCs was evaluated *in vitro* (Fig. 4). A previous study demonstrated that RBC ATP levels were markedly reduced (>50%) after incubation with ribavirin (1 mM) for 12 h (De Franceschi et al., 2000). In our study, washed RBCs were incubated with either **2** or ribavirin. RBCs treated with **2** displayed an ATP level nearly identical to the normalized control with the luminescence dropping only 3%. In contrast, the ribavirin-treated RBCs showed an approximately 73% reduction in ATP levels compared to the normalized control, a result consistent with previous reports (De Franceschi et al., 2000). These results indicate that **2** does not significantly reduce ATP levels and therefore is not readily metabolized to ribavirin and/or **1** in RBCs.

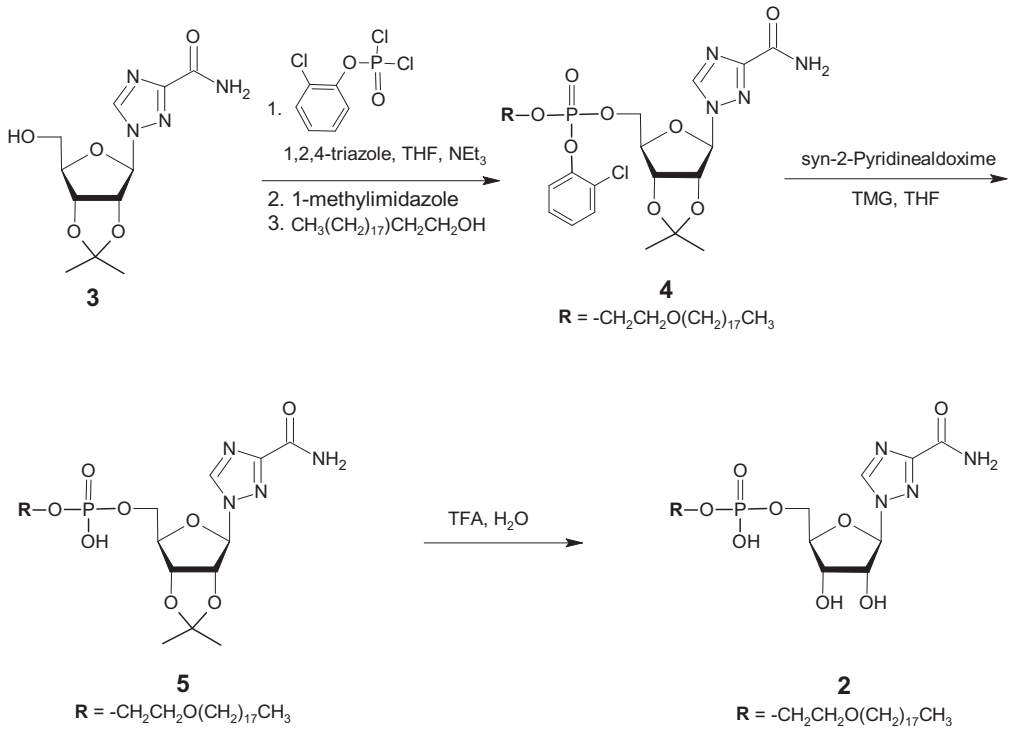

Fig. 2. Preparation of prodrug **2**. See text for details.

Table 1
In vitro antiviral activity of prodrug **2** versus ribavirin.

Virus	Compound	EC_{50} (μM) (SD)	CC_{50} (μM) (SD)	Selectivity index
HCV replicon (genotype 1b)	Ribavirin (**1**)	31 ± 3.5	76 ± 2.1	2.5
	Prodrug **2**	2.9 ± 0.5	182 ± 4.1	63
HCV replicon (genotype 1a)	Ribavirin (**1**)	38 ± 1.2	78 ± 1.1	2.1
	Prodrug **2**	6.3 ± 0.9	185 ± 3.2	29
Influenza A (HK strain H3N2)	Ribavirin (**1**)	37	>410	>11
	Prodrug **2**	0.5	66	132

HCV and influenza assays were performed in triplicate. Cytotoxicity assays were performed in triplicate for HCV and in duplicate for influenza. Values presented (± standard deviations [S.D.]) were calculated by linear regression analysis using data combined from all treated cultures. S.D. was calculated using the standard error of regression generated from the linear regression analyses (QuattroProTM). EC_{50}, drug concentration at which a 2-fold depression of HCV RNA (relative to the average levels in untreated cultures) or the minimum inhibitory drug concentration which reduces the CPE by 50%; CC_{50}, drug concentration at which a 2-fold depression of neutral red dye uptake (relative to the average levels in untreated cultures) was observed in AVA5 or APC103 cells or minimum toxic drug concentration which causes the reduction of viable MDCK cells by 50%.

3.2.4. In vitro uptake studies in RBCs and HepG2 cells

The uptake of **2** and ribavirin in RBCs was determined using radiolabeled analogs (Fig. 5) (Yeh et al., 2005; Lin et al., 2003). 5-[^{14}C]-ribavirin was rapidly transported from human plasma into RBCs with nearly 75% of the radioactivity partitioning into RBCs in just two hours. In the [^{14}C]-**2**-treated plasma, only approximately 7% of the radioactivity was transported over 4 h into RBCs, indicating that **2** is not readily taken up from plasma. It is possible that the lipophilic nature of the prodrug may cause it to be plasma protein bound which may contribute to the limited observed uptake into RBCs.

The uptake of **2** and ribavirin in the HepG2 human liver carcinoma cell line was then evaluated (Fig. 6). HepG2 cells were incubated with either [^{14}C]-**2** or 5-[^{14}C]-ribavirin for 24 h. The observed uptake levels of ribavirin in HepG2 cells were consistent with previously reported *in vitro* results using [^{3}H-]-ribavirin (Lau and Hong, 2004; Ibarra and Pfeiffer, 2009). The uptake level of **2** was more than 10-fold higher than ribavirin, suggesting that the prodrug is not solely dependent on ENT1 active transport. Based on the total radioactivity recovered, a significant amount of non-specific binding of **2** to the polystyrene plate (approximately 28%) was observed. Therefore, the observed uptake may only represent the lower limit of the actual uptake. The higher uptake of **2** in HepG2 cells is consistent with its improved antiviral efficacy as well as **2**'s improved effect on nucleotide pools.

3.3. In vivo studies

3.3.1. Plasma stability

Prior to *in vivo* evaluations, the stability of **2** was evaluated in rat plasma at 37 °C over 6 h (Supplementary Information). There was no trend of decreasing concentrations of **2** nor was there any detectable ribavirin over the course of the study, indicating that **2** was stable in rat plasma (data not shown).

3.3.2. 28-Day dosing in rats

To evaluate prodrug **2** *in vivo*, male Sprague Dawley rats were dosed orally either with **2** (304.8 mg/kg) or a molar equivalent dosage of ribavirin (120 mg/kg/day) once-daily for 28 consecutive days (Lin et al., 2003; Dadgostari et al., 2004). At these high doses,

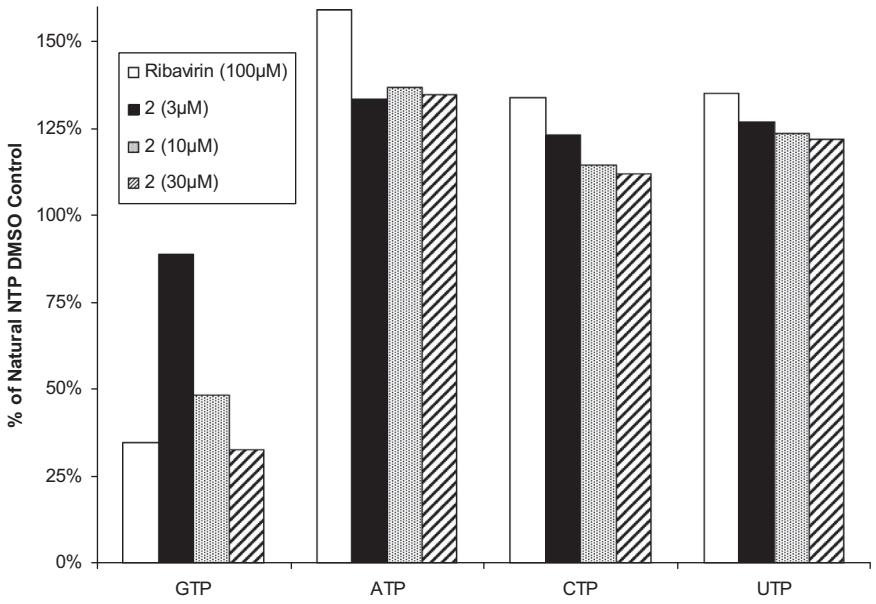

Fig. 3. The effect of prodrug **2** or ribavirin on cellular GTP and nucleotide pool levels in a whole-cell assay. Huh-7.5 cells were incubated with DMSO (vehicle control), ribavirin (positive control), or prodrug **2** for 24 h and then extracted to collect nucleotide triphosphate (NTP) pools. In a single experiment, HPLC was used to identify and quantify various NTP levels based on characteristic UV absorption spectra and retention times. Percent changes in the NTP peak areas of the treated samples relative to the NTP peak areas found in the DMSO control are shown for ribavirin (100 μM, white bar) and prodrug **2** at three different concentrations (3 μM, solid black bar; 10 μM, grey bar; 30 μM, cross-hatched bar). Two depleted GTP pools in a dose-dependent fashion but with modest effect on other NTP pools.

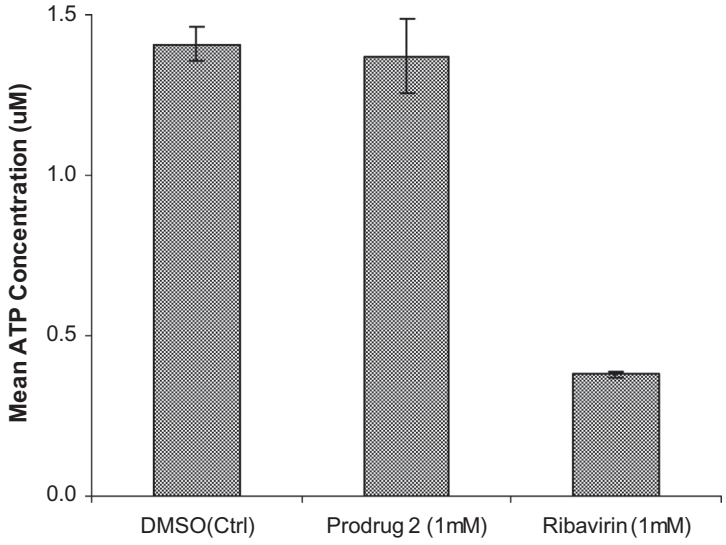

Fig. 4. The effect of prodrug **2**, ribavirin, or DMSO on ATP concentrations in RBCs. Washed RBCs were incubated with either DMSO vehicle control, prodrug **2** (1 mM), or ribavirin (1 mM) for 12 h and the resulting ATP levels were determined by CellTiter-Glo®. The experiment was performed in duplicate, and the DMSO control was normalized for ribavirin interference by adding ribavirin to the sample just prior to luminescence measurement. RBCs treated with two displayed an ATP level nearly identical to the normalized control. Ribavirin-treated RBCs showed an approximately 73% reduction in ATP levels (mean values are shown; error bars represent S.D.).

both prodrug **2** and ribavirin were generally well-tolerated and without mortality. Over the course of the study, lower body weights, lower body weight gains, and reduced food consumption were observed for both dosing groups. Plasma samples were collected at pre-dose and 1, 3, and 6 h post-dose on days 1, 14, and 28 after dosing. Plasma levels of **2** and ribavirin were determined simultaneously using a single LCMS/MS method (Supplementary Information). Following oral dosing of **2**, the prodrug was orally absorbed and increasing plasma levels were observed over time, reaching a maximum at 6 h (Fig. 7a). Modest levels of ribavirin derived from **2** were also observed, confirming that **2** converted to ribavirin *in vivo*. Over the course of the 28-day study, Areas Under the Curve ($AUC_{(0-24\ h)}$) for both plasma ribavirin and **2** were determined at days 1, 14, and 28 (Fig. 7b). In the control group receiving ribavirin, the plasma ribavirin $AUCs_{(0-24\ h)}$ were: 18,787; 16,267; and 19,958 ng•h/mL for days 1, 14, and 28, respectively, indicating that steady-state plasma levels of ribavirin were obtained following the first dose (Fig. 7b). In the group receiving prodrug **2**, the $AUCs_{(0-24\ h)}$ for **2** were similar for days 1, 14, and 28 (31,678; 30,323; 42,637 ng•h/mL), indicating that the **2** steady-state plasma $AUC_{(0-24\ h)}$ was reached immediately after the first dosage of **2** (Fig. 7b). For the group treated with **2**, the plasma ribavirin $AUCs_{(0-24\ h)}$ were: 5946; 33,140; and 48,942 ng•h/mL for days 1, 14, and 28 (Fig. 7b). Plasma ribavirin levels in the group receiving

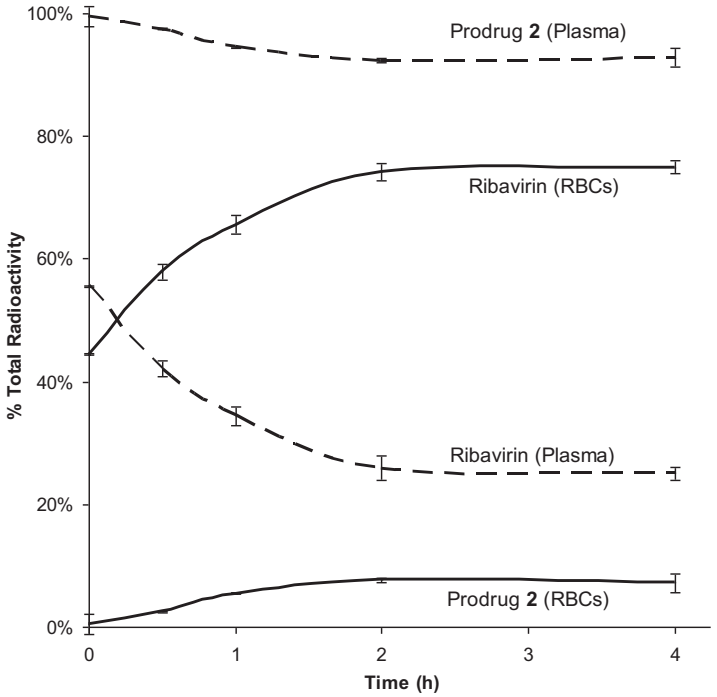

Fig. 5. The uptake of [^{14}C]-2 or 5-[^{14}C]-ribavirin into RBCs. Uptake was determined by spiking plasma with the radiolabeled test article and then combining with the blood cell suspension to achieve a target concentration of 100 μg (0.1 μCi)/mL in the reconstituted whole blood. Assays were performed in duplicate with three samples collected per timepoint (0, 0.5, 1, 2, and 4 h) following RBC separation from plasma by centrifugation. The percent total radioactivity in the RBCs (solid line) and plasma (dashed line) was determined by LSC (mean values are shown; error bars represent S.D.).

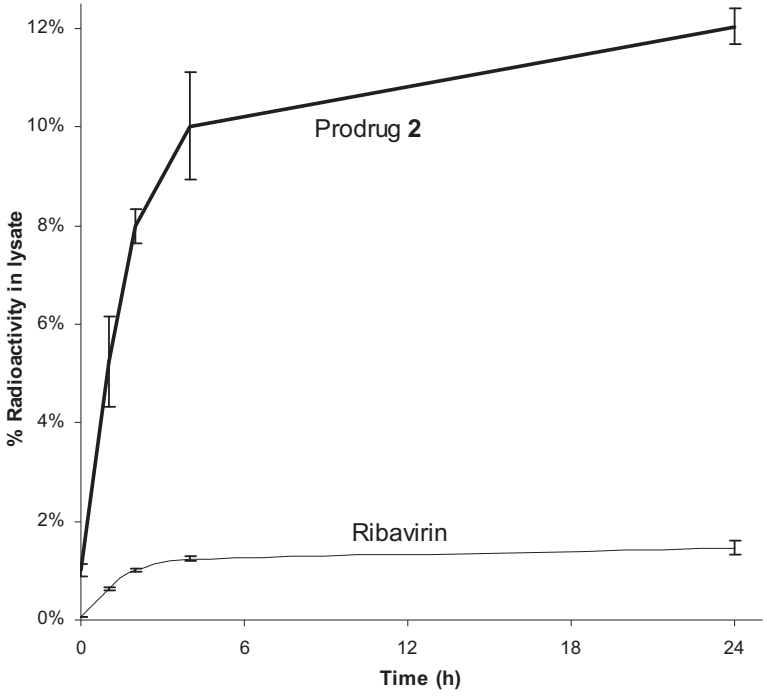

Fig. 6. The uptake of [^{14}C]-2 or 5-[^{14}C]-ribavirin into liver cells. HepG2 cells were incubated with either 100 μg (0.1 μCi)/mL [^{14}C]-2 or 5-[^{14}C]-ribavirin for 24 h. Assays were performed in duplicate with three samples per timepoint (0, 0.5, 1, 2, 4, and 24 h) followed by removal of supernatant, cold PBS wash of cells, and a total cell lysate preparation. The percent lysate radioactivity was determined by liquid scintillation counting (mean values are shown; error bars represent S.D.).

prodrug **2** increased and accumulated as a function of the administration duration. Overall, **2** yielded a 104% higher plasma ribavirin $AUC_{(0–24\ h)}$ on day 14 and 147% higher plasma ribavirin $AUC_{(0–24\ h)}$ on day 28 than that administrated with equivalent ribavirin control.

3.3.3. Tissue distribution

The tissue distribution of **2** and ribavirin was studied in male Sprague Dawley rats after a single oral dose of either [^{14}C]-**2** or 5-[^{14}C]-ribavirin (10 mg/kg). All animals exhibited normal behavior following dose administration and exhibited no overt signs of

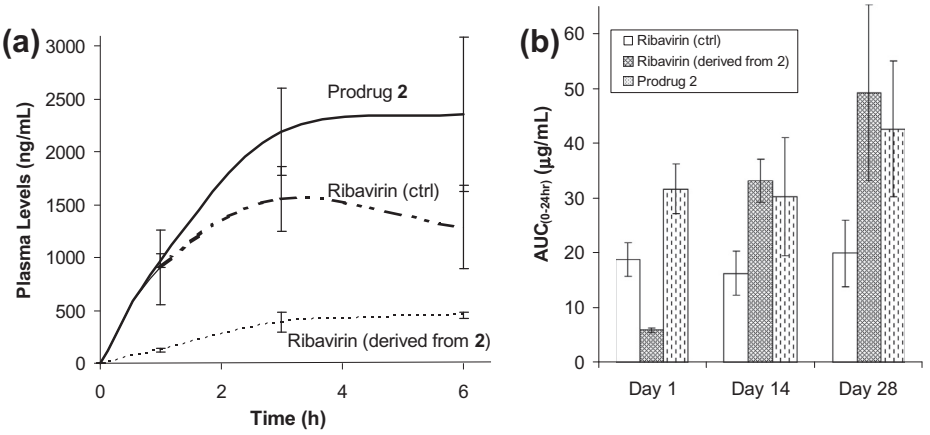

Fig. 7. The *in vivo* pharmacokinetic behavior of prodrug **2** and ribavirin. Sprague Dawley rats received equivalent molar dosages of either two (304.8 mg/kg) or ribavirin (120 mg/kg) by daily oral gavage for 28 consecutive days. The study was performed a single time with blood samples collected from three animals per timepoint per test article (prior to dose and at 1, 3, and 6 h post-dose) on days 1, 14, and 28. Plasma was analyzed by LC/MS/MS. (a) Day 1 plasma levels of prodrug **2** (solid line) and ribavirin derived from 2 (dashed line) in rats ($n = 6$) or plasma levels from the ribavirin control (alternating dashed line) in rats ($n = 6$) (mean values are shown; error bars represent S.D.). (b) Plasma $AUCs_{(0-24\ h)}$ for ribavirin control (solid white bars, $n = 22$); for ribavirin derived from two (cross-hatched bars, $n = 22$); for two (dashed line bars) on days 1, 14, and 28 (mean values are shown; error bars represent S.D.).

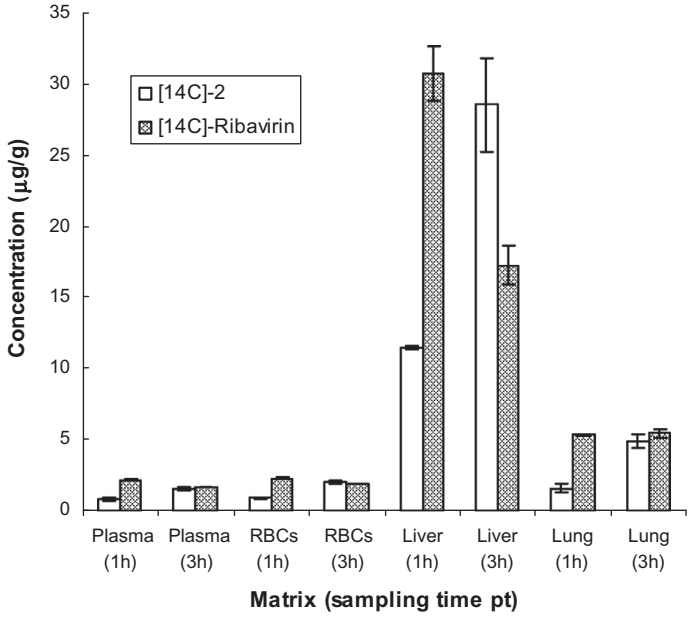

Fig. 8. The tissue distribution of total radioactivity derived from [^{14}C]-prodrug **2** or [^{14}C]-ribavirin. Sprague Dawley rats received a single dose (10 mg/kg) of either [^{14}C]-prodrug **2** (white bar, $n = 4$) or [^{14}C]-ribavirin (cross-hatched bar, $n = 4$) by oral gavage. The study was performed a single time with two animals per timepoint per test article (at 1 and 3 h post-dose). Following terminal sacrifice at 1 or 3 h, blood, liver, and lung samples were collected, and the plasma and RBCs separated by centrifugation. Duplicate aliquots from each homogenized sample where quantified by LSC to determine radioactivity concentrations (μg equivalent/g) in plasma, red blood cells, liver and lung at 1 and 3 h (mean values are shown; error bars represent S.D.).

toxicity throughout the study. Total radioactivity concentrations in plasma, RBCs, liver and lung at 1 and 3 h were determined by LSC (Fig. 8), but specific species such as **2**, **1**, ribavirin, and other metabolites were not explicitly identified in the study. For both **2** and ribavirin, liver exhibited the highest radioactivity concentrations followed by lung. After dosing of prodrug [^{14}C]-**2**, radioactivity concentrations approximately doubled from 1 to 3 h in all tissues, with liver radioactivity increasing from 11.5 μg equivalent/g at 1 h to 28.5 μg equivalent/g at 3 h. On the other hand, after [^{14}C]-ribavirin administration, radioactivity concentrations decreased from 1 to 3 h in all tissues except for lung which remained steady. In particular, the liver radioactivity decreased from 29.4 μg equivalent/g at 1 h to 18.2 μg equivalent/g at 3 h. These data are consistent with the pharmacokinetic study results (Fig. 7a) wherein peak concentrations for prodrug **2** were observed at approximately 4–6 h, but earlier for ribavirin (3 h). Assuming that liver radioactivity at 3 and 24 h were similar, the estimated liver $AUC_{(0-24\ h)}$'s for prodrug **2** and ribavirin were calculated to be 644 and 445 μg equivalent/g•h, respectively, suggesting that **2** could achieve substantially higher liver radioactivity levels than ribavirin after a single oral dose. The potential for increased liver exposure suggests that prodrug **2** could be administered at a much lower dose than ribavirin yet still achieve liver levels necessary for activity while significantly reducing the exposure to RBCs.

4. Discussion

Compound **2** represents a novel approach toward a ribavirin prodrug with potentially superior antiviral activity and better tolerability characteristics. The *in vitro* data suggest that the phosphodiester prodrugging approach can successfully deliver and subsequently release active ribavirin mono-phosphate **1** in nucleated cells such as hepatocytes. Consequently, **2** is more active than ribavirin against HCV and influenza virus as well as more effective in depleting guanine nucleotide pools. In anucleated RBCs, prodrug **2** has minimal impact on ATP levels and limited uptake. Conversely, prodrug **2** has much higher uptake levels in nucleated HepG2 hepatocytes consistent with its improved activity against the HCV replicon. The improved uptake observed of **2** in HepG2 cells suggests a possible approach to overcoming the variability of ribavirin hepatocytic uptake in the broader patient population with chronic HCV infection by avoiding sole reliance on the variable uptake capacities of different ENT1 isoforms.

In vivo studies indicate that the prodrug **2** is orally bioavailable and well tolerated. Unlike ribavirin which achieves steady-state equilibrium plasma levels quickly, uptake of prodrug **2** was slower in rats but continued accumulating compared to the ribavirin control (Fig. 7b). When dosed at a molar equivalent level to ribavirin, because of its different accumulation profile, prodrug **2** produced plasma $AUC_{(0-24\ h)}$ levels of ribavirin over the span of the 28-day study that exceeded the levels derived from the ribavirin control. At the same time, tissue distribution studies (Fig. 8) show that prodrug **2** radioactivity levels in the liver significantly surpass those generated from the ribavirin control when both compounds were administered at equal doses. When administered at molar equivalent dosages over long periods, prodrug **2** may produce plasma ribavirin levels similar to ribavirin, which could limit some of the safety potential advantages of the prodrug at this dose. However, because of prodrug **2**'s greater antiviral activity and better liver distribution, these data suggest **2** could potentially be administered at a fraction of the conventional ribavirin dosage thereby minimizing RBC exposure yet still achieving liver levels of the active phosphorylated species similar to ribavirin. Additionally, the higher uptake and accumulation of prodrug **2** suggest that it could also be dosed less frequently than ribavirin, which must be administered from 500 to 600 mg twice a day, every day, during treatment of hepatitis C.

As new therapeutic modalities for HCV infection arise, there is likely to be continued interest in complementary ribavirin analogs that have less variability in both efficacy and dosing and can be more readily combined with other antivirals (Paeshuyse et al., 2011; Vermehren and Sarrazin, 2011). Future work will examine **2**'s efficacy compared to a ribavirin control in relevant *in vivo* models such as the murine influenza model, as well as optimizing dosing regimens to define further the potentially larger therapeutic window between activity and toxicity (Matsuoka et al., 2009).

Acknowledgments

We gratefully acknowledge Drs. Vaishali Chaudhuri and Howard J. Worman for critically reviewing this manuscript.

Appendix A. Supplementary data

Supplementary data associated with this article can be found, in the online version, at http://dx.doi.org/10.1016/j.antiviral.2013.04.014.

References

Bengsch, B., Thimme, R., 2010. Ribavirin ante portas: uptake transporters into hepatocytes dissected. J. Hepatol. 52, 469–471.
Blight, K.J., Kolykhalov, A.A., Rice, C.M., 2000. Efficient initiation of HCV RNA replication in cell culture. Science 290, 1972–1974.
Crotty, S., Cameron, C., Andino, R., 2002. Ribavirin's antiviral mechanism of action: lethal mutagenesis? J. Mol. Med 80, 86–95.
Dadgostari, S., Xu, C., Yeh, L.-T., Lin, C.C., Vitarella, D., 2004. Viramidine demonstrates better safety than ribavirin in monkeys but not rats. Drug. Chem. Toxicol. 27, 191–211.
De Franceschi, L., Fattovich, G., Turrini, F., Ayi, K., Brugnara, C., Manzato, F., Noventa, F., Stanzial, A.M., Solero, P., Corrocher, R., 2000. Hemolytic anemia induced by ribavirin therapy in patients with chronic hepatitis C virus infection: role of membrane oxidative damage. Hepatology 31, 997–1004.
Di Pierro, D., Tavazzi, B., Perno, C.F., Bartolini, M., Balestra, E., Caliò, R., Giardina, B., Lazzarino, G., 1995. An ion-pairing high-performance liquid chromatographic method for the direct simultaneous determination of nucleotides, deoxynucleotides, nicotinic coenzymes, oxypurines, nucleosides, and bases in perchloric acid cell extracts. Anal. Biochem. 231, 407–412.
Dixit, N.M., Perelson, A.S., 2006. The metabolism, pharmacokinetics and mechanisms of antiviral activity of ribavirin against hepatitis C virus. Cell. Mol. Life Sci. 63, 832–842.
Feld, J.J., 2012. Is there a role for ribavirin in the era of hepatitis C virus direct-acting antivirals? Gastroenterology 142, 1356–1359.
Fletcher, T., Ptak, R., Bartram, S., Halliday, S., Buckheit, R., Moravec, R., Riss, T., 2000. A HTS system for screening antiviral compounds using the cell Titer® 96 aqueous one solution assay. Promega Notes 75, 13–16.
Fukuchi, Y., Furihata, T., Hashizume, M., Iikura, M., Chiba, K., 2010. Characterization of ribavirin uptake systems in human hepatocytes. J. Hepatol. 52, 486–492.
He, G.-X., Krise, J.P., Oliyai, R., 2007. Prodrugs of phosphonates, phosphinates, and phosphates. In: Stella, V.J., Borchardt, R.T., Hageman, M.J., Oliyai, R., Maag, H., Tilley, J.W. (Eds.), Prodrugs. Springer, New York, NY, pp. 923–964.
Hostetler, K.Y., Beadle, J.R., Hornbuckle, W.E., Bellezza, C.A., Tochkov, I.A., Cote, P.J., Gerin, J.L., Korba, B.E., Tennant, B.C., 2000. Antiviral activities of oral 1-O-hexadecylpropanediol-3-phosphoacyclovir and acyclovir in woodchucks with chronic woodchuck hepatitis virus infection. Antimicrob. Agents Chemother. 44, 1964–1969.
Hostetler, K.Y., Rybak, R.J., Beadle, J.R., Gardner, M.F., Aldern, K.A., Wright, K.N., Kern, E.R., 2001. *In vitro* and *in vivo* activity of 1-O-hexadecylpropanediol-3-phosphoganciclovir and 1-O-hexadecylpropanediol-3-phospho-penciclovir in cytomegalovirus and herpes simplex virus infections. Antivir. Chem. Chemother. 12, 61–70.
Hostetler, Karl Y., 2009. Alkoxyalkyl prodrugs of acyclic nucleoside phosphonates enhance oral antiviral activity and reduce toxicity: current state of the art. Antiviral Res. 82, A84–98.
Hostetler, Karl Y., 2010. Synthesis and early development of hexadecyloxypropyl-cidofovir: an oral antipoxvirus nucleoside phosphonate. Viruses 2, 2213–2225.
Ibarra, K.D., Pfeiffer, J.K., 2009. Reduced ribavirin antiviral efficacy via nucleoside transporter-mediated drug resistance. J. Virol. 83, 4538–4547.
Iikura, M., Furihata, T., Mizuguchi, M., Nagai, M., Ikeda, M., Kato, N., Tsubota, A., Chiba, K., 2012. ENT1, a ribavirin transporter, plays a pivotal role in antiviral efficacy of ribavirin in a hepatitis C virus replication cell system. Antimicrob. Agents Chemother. 56, 1407–1413.
Inoue, Y., Homma, M., Matsuzaki, Y., Shibata, M., Matsumura, T., Ito, T., Kohda, Y., 2006. Erythrocyte ribavirin concentration for assessing hemoglobin reduction in interferon and ribavirin combination therapy. Hepatol. Res. 34, 23–27.
Korba, B.E., Gerin, J.L., 1992. Use of a standardized cell culture assay to assess activities of nucleoside analogs against hepatitis B virus replication. Antiviral Res. 19, 55–70.
Lau, J., Hong, Z., 2004. Methods of drug delivery to hepatocytes and treatment of flaviviridae infections [WWW Document]. <http://patentscope.wipo.int/search/en/WO2002015904> (accessed 5.23.12).
Lin, C., Yeh, L.-T., Vitarella, D., Hong, Z., 2003a. Viramidine, a prodrug of ribavirin, shows better liver-targeting properties and safety profiles than ribavirin in animals. Antivir. Chem. Chemother. 14, 145–152.
Lin, C.-C., Luu, K., Lourenco, D., Yeh, L.-T., 2003b. Pharmacokinetics and metabolism of [^{14}C]viramidine in rats and cynomolgus monkeys. Antimicrob. Agents Chemother. 47, 2458–2463.
Matsuoka, Y., Lamirande, E.W., Subbarao, K., 2009. The mouse model for influenza. In: Coico, R., Kowalik, T., Quarles, J., Stevenson, B., Taylor, R. (Eds.), Current Protocols in Microbiology. John Wiley & Sons, Inc., Hoboken, NJ, USA.
Okuse, C., Rinaudo, J.A., Farrar, K., Wells, F., Korba, Brent.E., 2005. Enhancement of antiviral activity against hepatitis C virus *in vitro* by interferon combination therapy. Antiviral Res. 65, 23–34.
Paeshuyse, J., Dallmeier, K., Neyts, J., 2011. Ribavirin for the treatment of chronic hepatitis C virus infection: a review of the proposed mechanisms of action. Curr. Opin. Virol. 1, 590–598.
Page, T., Connor, J.D., 1990. The metabolism of ribavirin in erythrocytes and nucleated cells. Int. J. Biochem. 22, 379–383.
Parker, W.B., 2005. Metabolism and antiviral activity of ribavirin. Virus Res. 107, 165–171.

Pockros, P.J., 2010. New direct-acting antivirals in the development for hepatitis C virus infection. Therap. Adv. Gastroenterol. 3, 191–202.
Randall, G., Grakoui, A., Rice, Charles M., 2003. Clearance of replicating hepatitis C virus replicon RNAs in cell culture by small interfering RNAs. PNAS 100, 235–240.
Russmann, S., Grattagliano, I., Portincasa, P., Palmieri, V.O., Palasciano, G., 2006. Ribavirin-induced anemia: mechanisms, risk factors and related targets for future research. Curr. Med. Chem. 13, 3351–3357.
Selle, H., Chapman, B.E., Kuchel, P.W., 1992. Release of choline by phospholipase D and a related phosphoric diester hydrolase in human erythrocytes. ^{1}H spin-echo n.m.r. studies. Biochem. J. 284 (Pt. 1), 61–65.
Shiffman, M.L., 2009. What future for ribavirin? Liver Int. 29 (Suppl. 1), 68–73.
Sidwell, R.W., Huffman, J.H., Khare, G.P., Allen, L.B., Witkowski, J.T., Robins, R.K., 1972. Broad-spectrum antiviral activity of Virazole: 1-beta-D-ribofuranosyl-1,2,4-triazole-3-carboxamide. Science 177, 705–706.
Vermehren, J., Sarrazin, C., 2011. New HCV therapies on the horizon. Clin. Microbiol. Infect. 17, 122–134.
Yeh, L.-T., Nguyen, M., Lourenco, D., Lin, C.-C., 2005. A sensitive and specific method for the determination of total ribavirin in monkey liver by high-performance liquid chromatography with tandem mass spectrometry. J. Pharm. Biomed. Anal. 38, 34–40.